Light-Dressing Effect in Laser-Assisted Elastic Electron Scattering by Xe

Y. Morimoto, R. Kanya, and K. Yamanouchi, PRL**115**, 123201(2015)

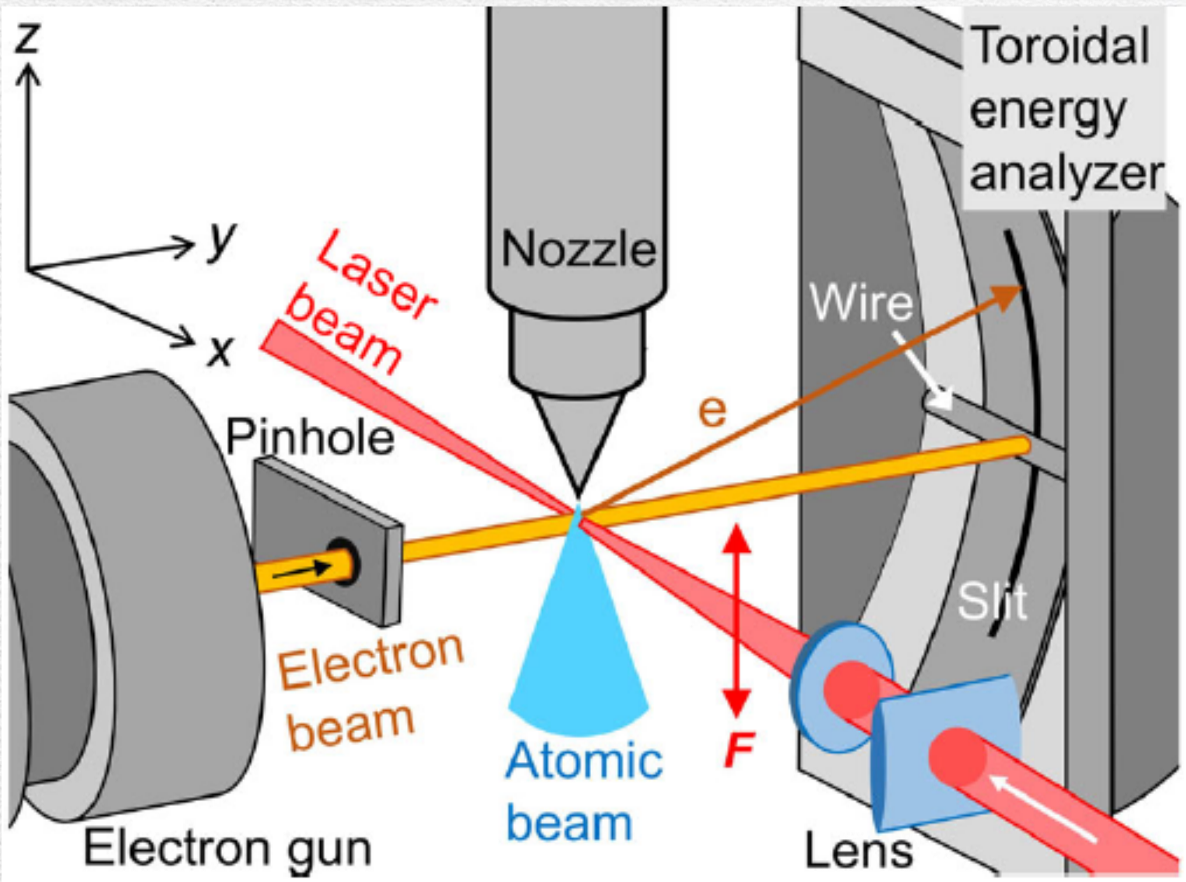

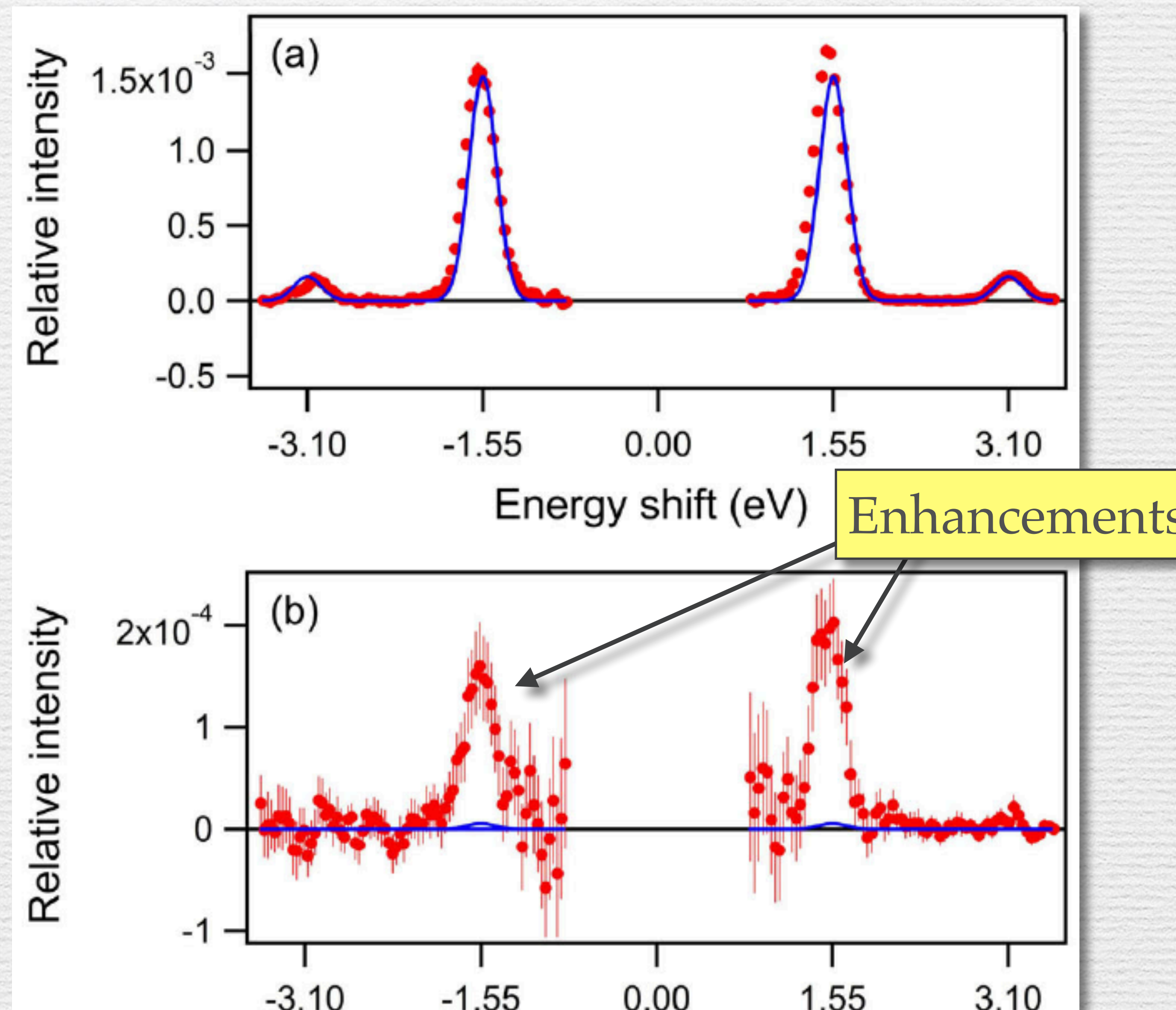

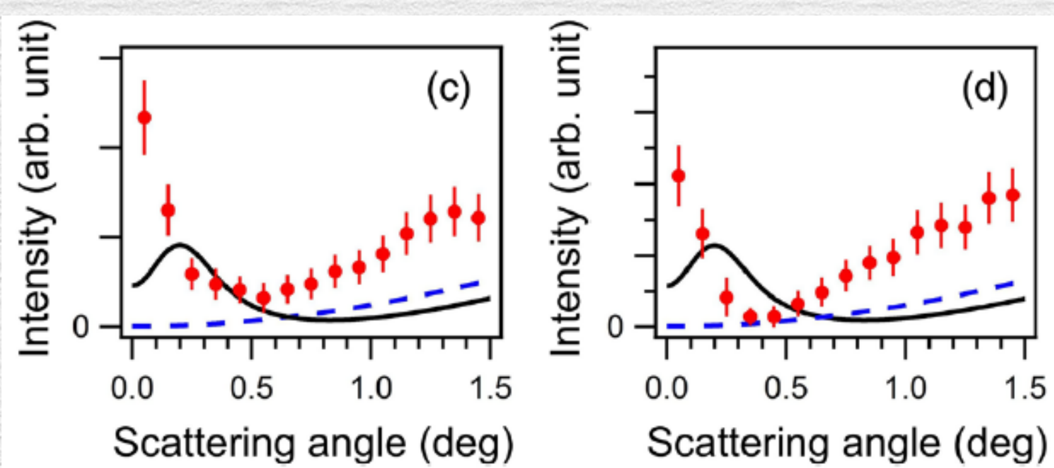

RCNP核理1aグループ勉強会 2018.11.15 by A. Tamii

Abstract

Y. Morimoto, R. Kanya, and K. Yamanouchi, PRL**115**, 123201(2015)

Light-Dressing Effect in Laser-Assisted Elastic Electron Scattering by Xe

Yuya Morimoto, Reika Kanya, and Kaoru Yamanouchi*

Department of Chemistry, School of Science, The University of Tokyo,
7-3-1, Hongo, Bunkyo-ku, Tokyo 113-0033, Japan

(Received 26 February 2015; published 16 September 2015)

The light-dressing effect in Xe atoms was identified in laser-assisted elastic electron scattering (LAES) signals. In the angular distribution of LAES signals with energy shifts of $\pm\hbar\omega$ recorded by the scattering of 1 keV electrons by Xe in an intense nonresonant laser field, a peak profile appeared at small scattering angles (<0.5°). This peak was interpreted as evidence of the light dressing of Xe atoms induced by an intense laser field on the basis of a numerical simulation in which the light-dressing effect is included.

DOI: 10.1103/PhysRevLett.115.123201 PACS numbers: 34.80.Qb

Key points of the discussions

Backgrounds:

Laser-assisted elastic electron scattering (LAES) is studied from 1970's

Developments

The authors developed a LAES measurement with a high-frequency (795nm) short pulse (50 fs) laser [37], and the measurement at very small scattering angles (this publication).

Achievements:

Light-dressing effect of the target atom has been firstly observed at the small scattering angle of 0.2°.

Applications:

Ultrafast (~10fs) gas electron diffraction for studying *e.g.* transient geometrical structures of molecules during chemical reactions.

Laser-assisted elastic electron scattering (LAES)

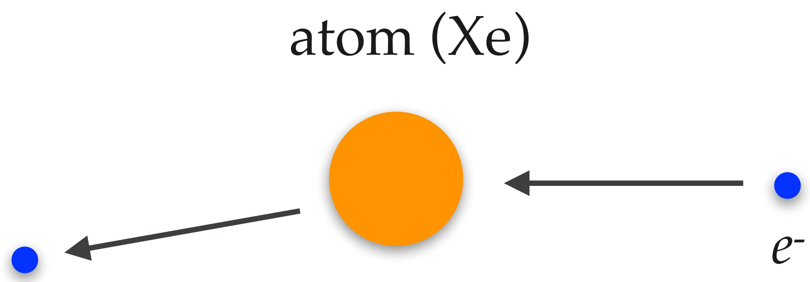

scattering in the free space

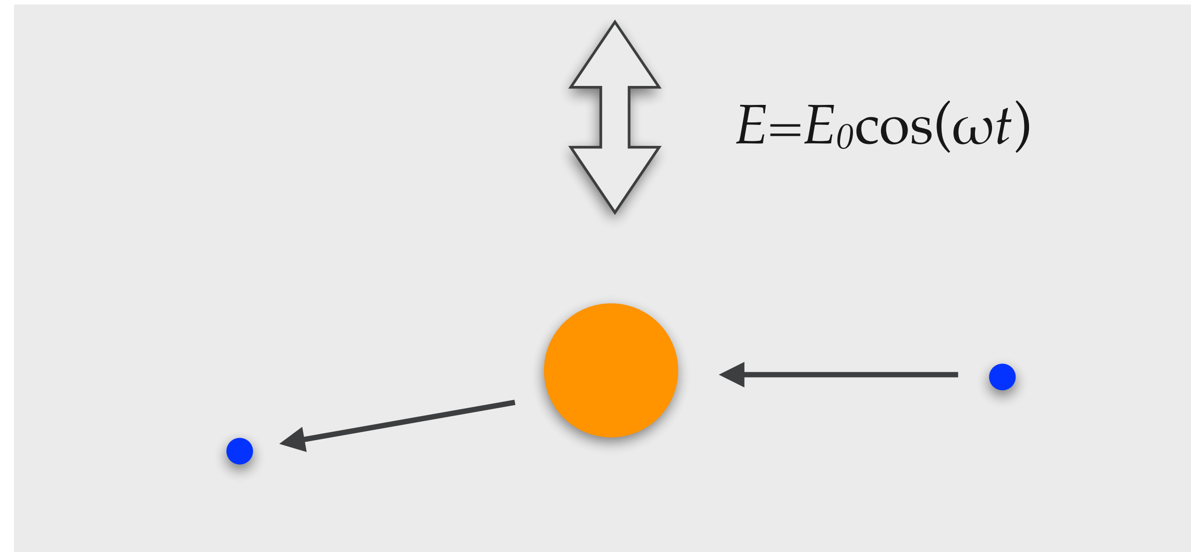

scattering in the laser field

The first principal effect observed in "LAES"

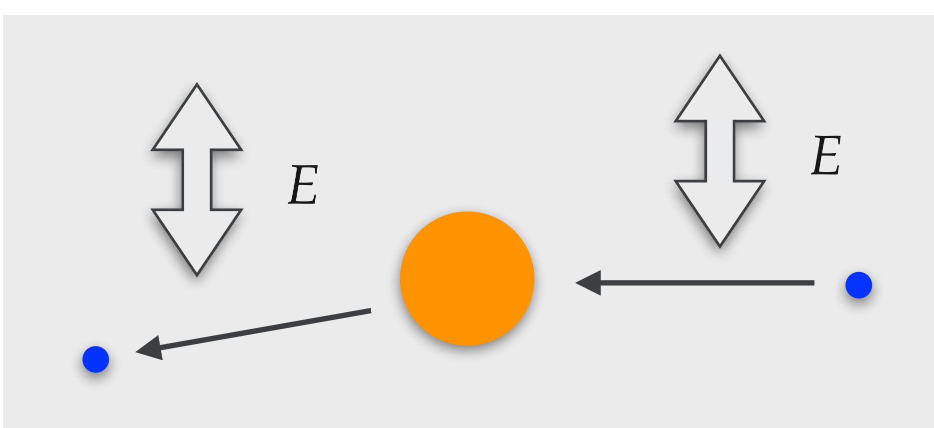

electron modulation by the laser

= light-dressed electrons

Gordon-Volkov wave

(in the infinite boundary)

calc. KW=Kroll-Watson [6]

The second principal effect

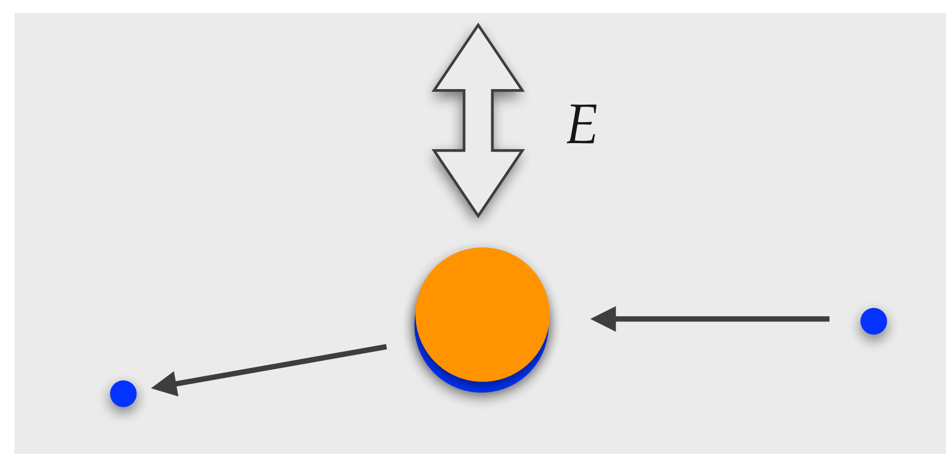

atomic polarization

= light-dressed atom

calc. Zon [38]

Electron modulation by the laser field

Kroll-Watson [6]

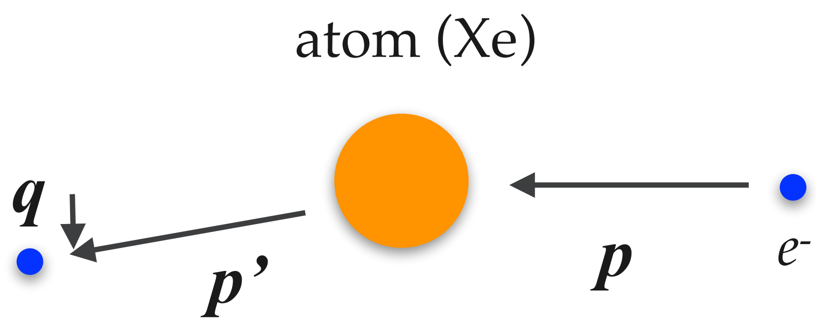

$$q = p' - p$$

$$\mathbf{A}(t) = \mathbf{A}_0 \cos(\omega t)$$

$$E = E_0 \cos(\omega t)$$

at $\alpha = \omega t = 0$

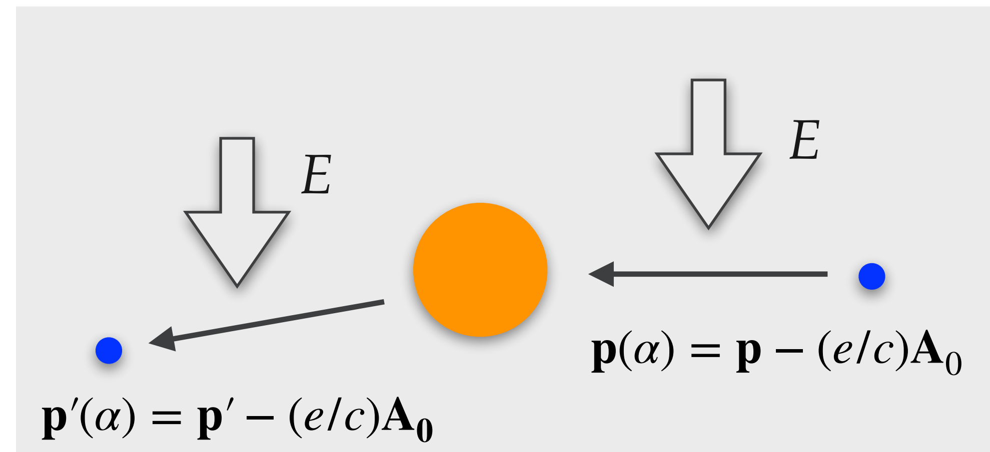

In the classical formalism

The instantaneous momentum transfer is

$$\mathbf{p}'(\alpha) - \mathbf{p}(\alpha) = \mathbf{p}' - \mathbf{p} = \mathbf{q}$$

at $\alpha = \omega t = \pi$

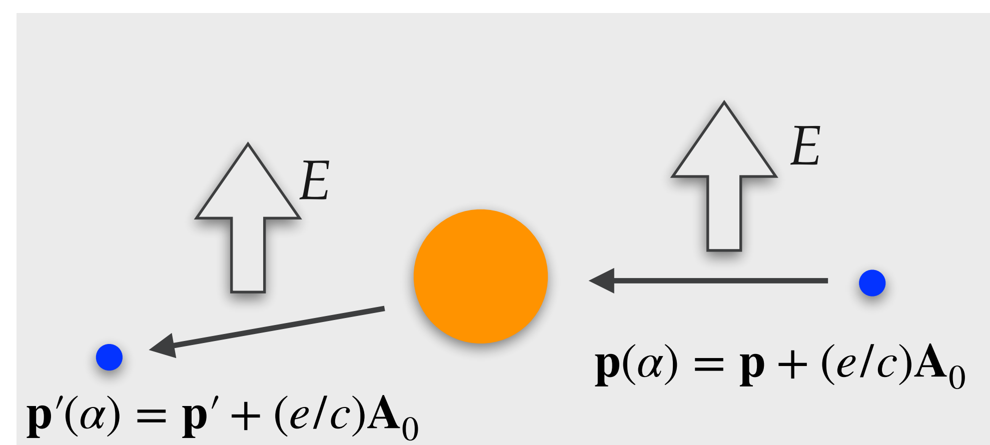

However, the energy difference is

$$\frac{1}{2m}(\mathbf{p}'^2(\alpha) - \mathbf{p}^2(\alpha)) = \frac{1}{2m}(\mathbf{p}'^2 - \mathbf{p}^2) - (e/mc)\mathbf{q} \cdot \mathbf{A}_0 \cos(\omega t)$$

The scattered electrons gain (or lose) energy depending on the laser phase.

Low-frequency condition:
the laser oscillation time ($1/\omega$) is much slower than the e-atom interaction time

In the quantum mechanics

Mason [4]

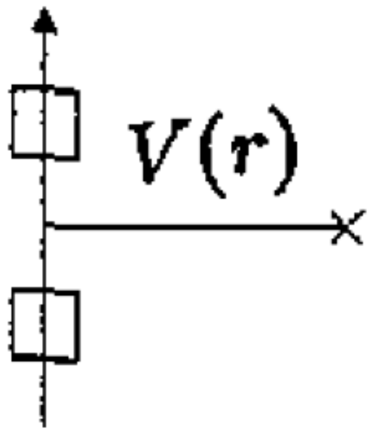

Electron modulated by the laser field in LAES

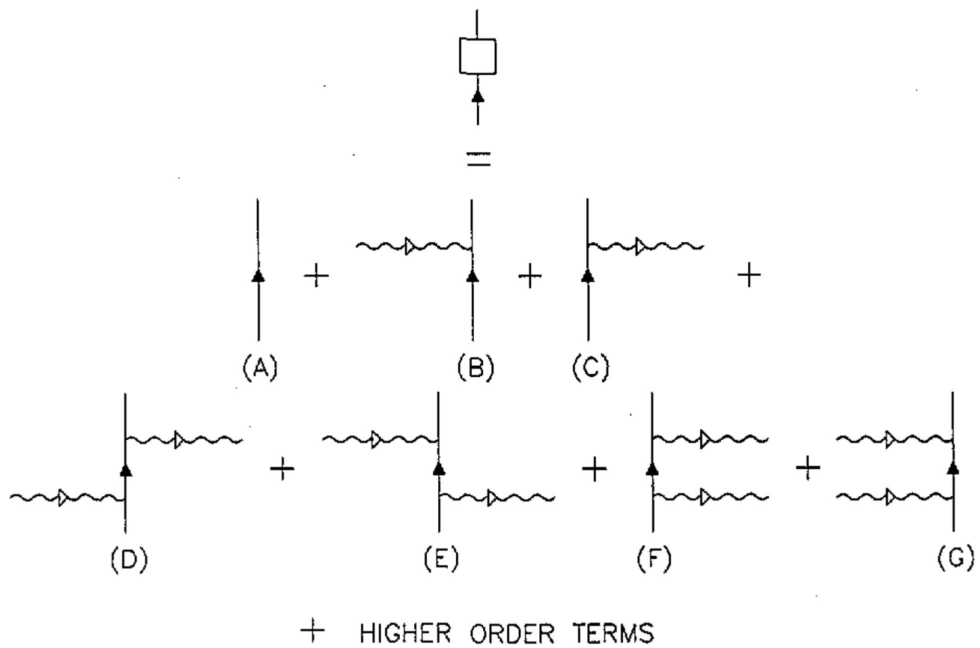

(A) free propagation

(B) photo-absorption = inverse Bremsstrahlung

(C) stimulated photo-emission = Bremsstrahlung

$$\frac{1}{2m}\left(\frac{\hbar}{i}\vec{\nabla}-\frac{e}{c}\vec{A}\right)^2\Psi+V\Psi=i\hbar\dot{\Psi}\,. \quad (3.1)$$

Kroll-Watson [6]

$$\Psi=\exp\left(-\frac{i}{\hbar}\int^t\frac{e^2}{2mc^2}A^2\,dt'\right)\varphi(t)\,. \quad (3.2)$$

Solution of φ for *V*=0

$$X_{\vec{k}}=e^{i\vec{k}\cdot\vec{r}}\exp\left[-\frac{i\hbar}{2m}\int^t\left(k^2-\frac{2e}{c\hbar}\vec{k}\cdot A\right)dt'\right] \quad (3.4)$$

Gordon-Vorkov
in the non-rel. formalism

In the quantum mechanics

Kroll-Watson[6]

in the first order Born approximation

$$\frac{d\sigma_n^{KW}}{d\Omega} = \frac{|p_{f,n}|}{|p_i|} J_n^2(\xi) \frac{d\sigma_{el}^{free}}{d\Omega}$$

Differential cross section for electrons modulated by the laser field is modified from the one in the free space for each of the n-photon absorption (or emission for negative n) process.

$$\xi = \frac{e\vec{E}_0 \cdot \vec{q}_n}{m_e \hbar \omega^2}$$

Order parameter

ξ>>1: classical limit

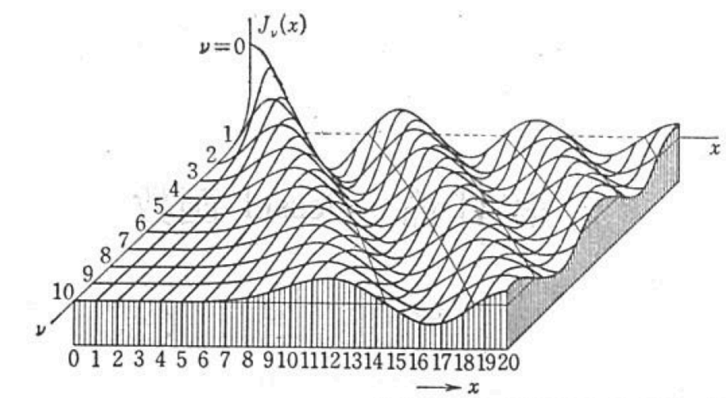

第 6.1 図　$J_\nu(x)$ を ν, x 2 変数の函数とみた立体模型

Bessel function of the first kind for the integer ν

$$\sum_{n=-\infty}^{\infty} \frac{d\sigma_n^{KW}}{d\Omega} = \frac{d\sigma_{el}^{free}}{d\Omega}$$

Sum-rule (when $p_f = p_i$)

<u>No additional information on the target atom can be obtained</u> comparing with the free-space scattering case. This is coming from the assumption of the calculation.

$$J_{-n}(\xi) = (-1)^n J_n(\xi)$$

J^2 is symmetric with respect to the sign of n

Light dressing atom

Zon [38]

electron modulation +

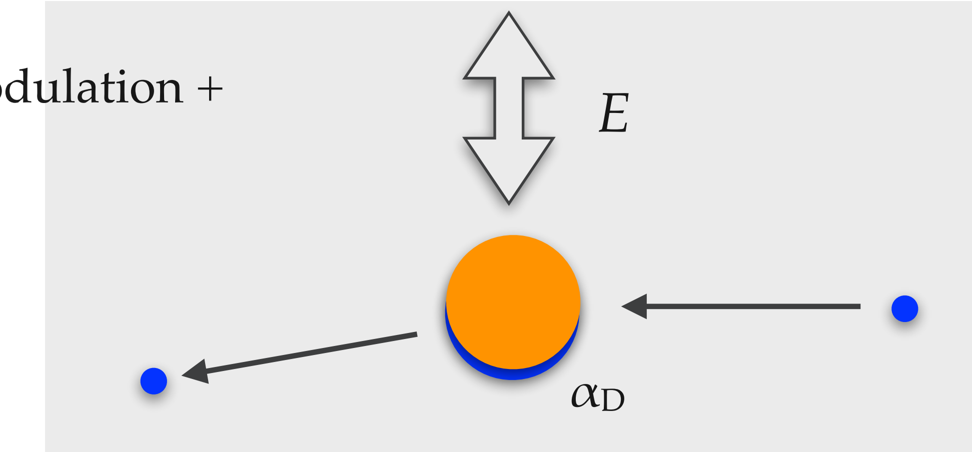

in the first order Born approximation

$$\frac{d\sigma_n^{Zon}}{d\Omega} = \frac{|p_{f,n}|}{|p_i|} |J_n(\xi) f_{el}^{free} - \frac{\alpha_D m_e^2 \omega^2 \xi}{2\pi\epsilon_0 q_n^2} J_n'(\xi)|^2$$

including the first order effect from the target atomic structure with the electric dipole polarizability (α_D)

α_D(Xe-atom) = 4.04Å^3

The effect may appear in the very forward scattering angle, i.e. q~0

$$\xi = \frac{e\vec{E}_0 \cdot \vec{q}_n}{m_e \hbar \omega^2}$$

$$x = \frac{\alpha_D m_e^2 \omega^2}{2\pi\epsilon_0 q_n^2}$$

In the electron-atom collision case

1 keV (32 keV/c), 0.2° (4mr)
q = 0.13 keV/c
$\hbar\omega$ = 1.55 eV

1.5×10^{12} W/cm^2 → 3.4×10^9 V/m

$\xi = 0.07$

$x = 4\times10^{-8}$ m

$(x\xi)^2 = 8\times10^{-18}$ m^2

LAES fraction is ~10^{-3}

Laser-assisted elastic electron scattering (LAES) [1-3]

The kinetic energy of the scattered electron changes by multiples of photon energy $n\hbar w$.

Kroll and Watson: formula (LAES without laser-atom interaction) [6]

$\rightarrow$ No information on the atom can be obtained [7]

Light-dressing effect in the LAES process

Gersten and Mittleman (1976) [8]

DCS of the LAES process with energy shift of $n\hbar\omega$

Time-dependent perturbation theory, Byron and Joachain [9]

Peak structure at small scattering angles in DCS for $\pm\hbar\omega$ also in [10,11]

$\rightarrow$ electron density distribution in a target atom influenced by an external laser field

Bessel Function of the First Kind

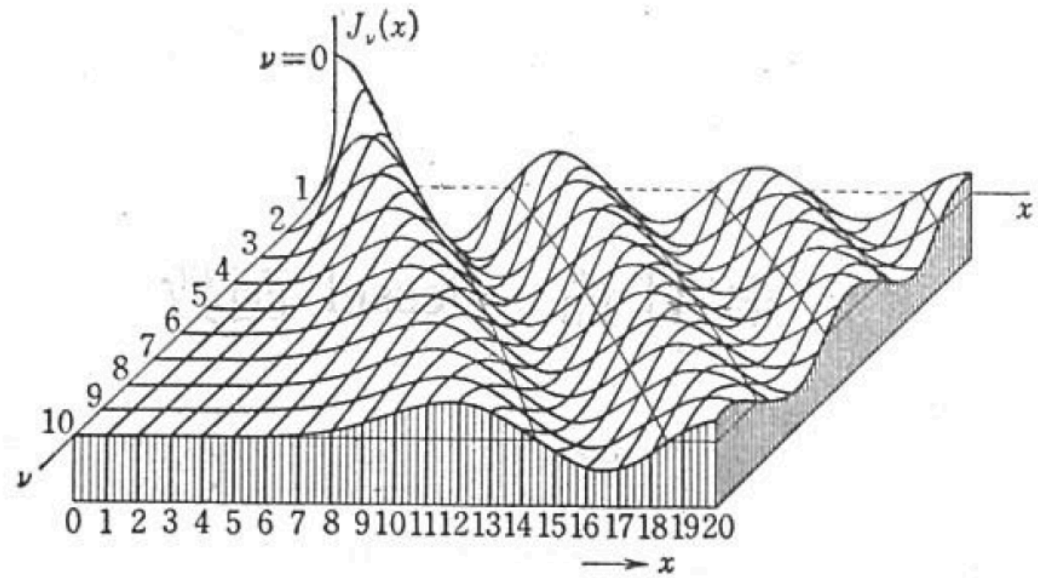

第6.1図　$J_\nu(x)$ を ν, x 2 変数の函数とみた立体模型

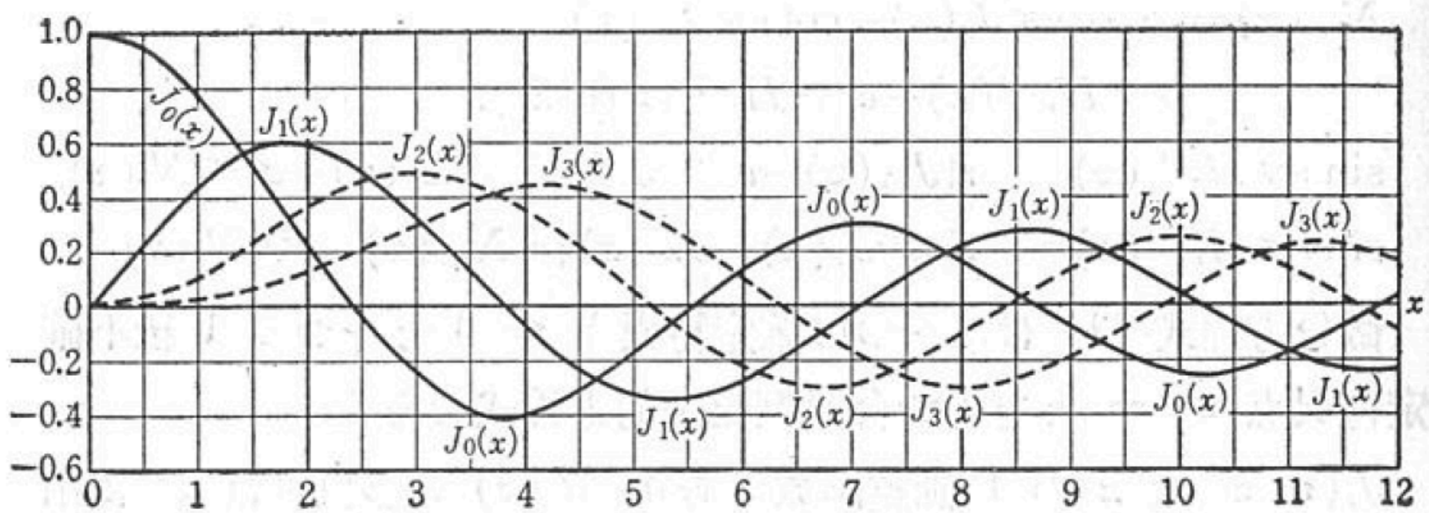

第6.2図　$J_0(x)$, $J_1(x)$, $J_2(x)$, $J_3(x)$ のグラフ

Experimental Setup

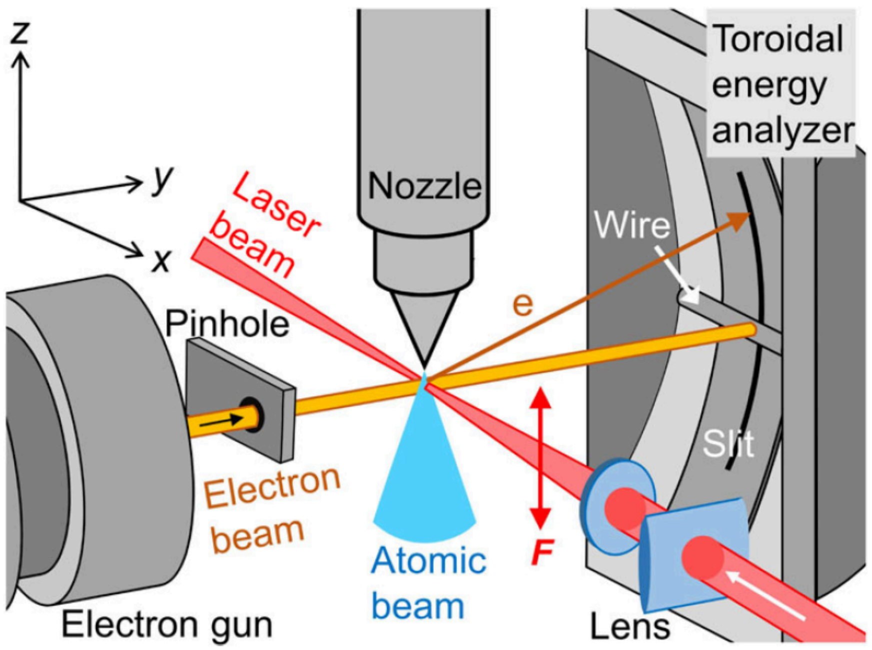

FIG. 1 (color online). Schematic of the experimental setup.

PRL115, 123201(2015)

R. Kanya et al., RSI82_124105(2011)

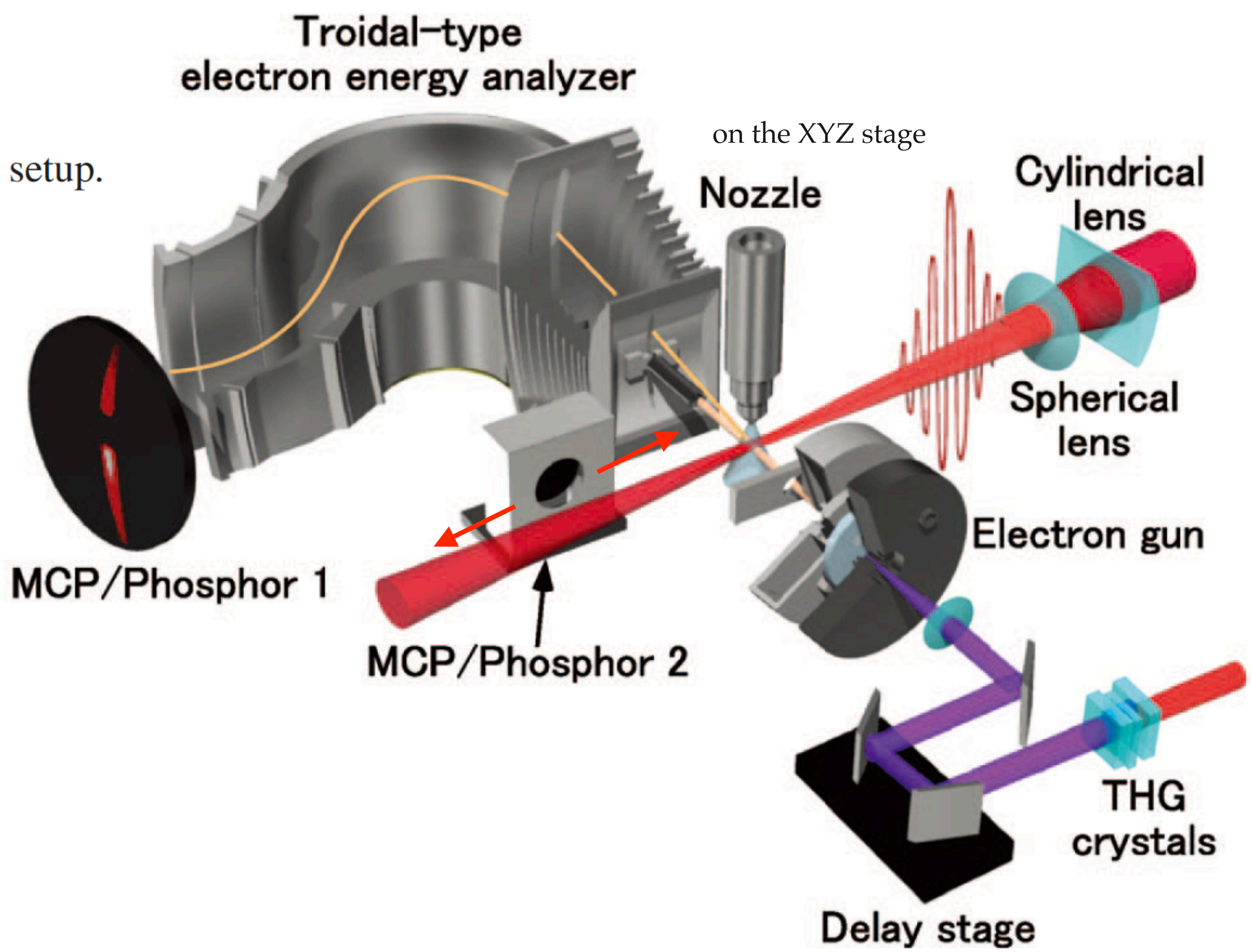

FIG. 1. (Color online) The schematic of the experimental setup of LAES.

Experimental Setup

numbers in RSI2011
numbers in PRL2015+Suppl.

Laser

Ti:Sapphire Laser
795 nm
0.44 mJ/pulse — 0.6 mJ/pulse
50 fs — 970(50) fs
5 kHz

linearly polarized
1.4×10^{12} W/cm^2 — $1.5(4)\times10^{12}$ W/cm^2

1.0 mm$^V\times$0.52 mm^H (FWHM)

0.12(3) mm$^V\times$0.81(5) mm^H

Gas beam

Xe gas
nozzle 0.5 mmϕ
Width: 1.3 mm (FWHM)
S.P. is at 0.4 mm below the nozzle

Electron Beam

photocathode: quartz coated with silver (50nm^t) — gold (10nm^t)

laser pulse: 267 nm (THG), 45 ps, 200pJ/pulse

pulse length: 0.8 mm (FWHM) on target

1 keV (acceleration in 0.3 mm gap), ⊿E~0.7 eV
< 10^3 electrons/pulse

slits: 1) 0.5mmϕ at 3.0mm 2) 0.7mmϕ at 35? mm
0.1mm

focus by electromagnetic lens (120mA×1000turn)

0.12±0.01 mmϕ (FWHM) at 20 mm downstream from the S.P.
measured by MCP/Phosphor2
0.23±0.01 mmϕ (FWHM) at the scattering point — 0.24(1) mm

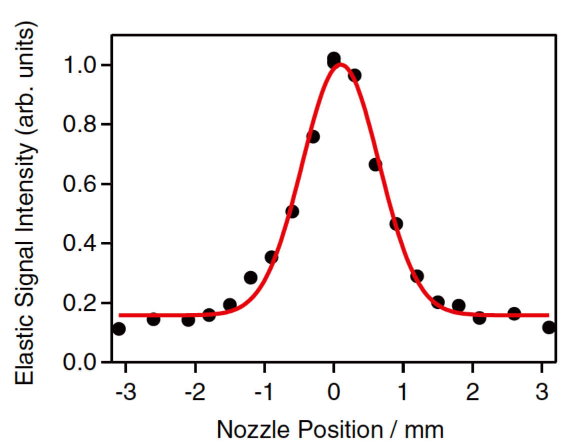

FIG. 2. (Color online) The nozzle-position dependence of the electron signal intensity of elastic scattering by Xe. Filled circles: Experimental results. Solid line: A fitting curve with a Gaussian function.

scan with moving the horizontal nozzle position

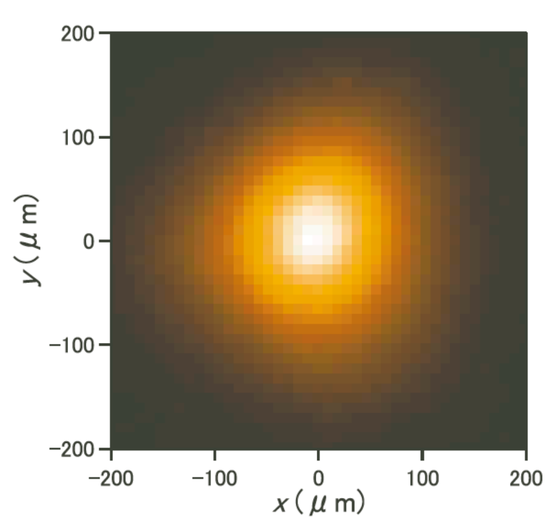

FIG. 4. (Color online) The electron beam profile.

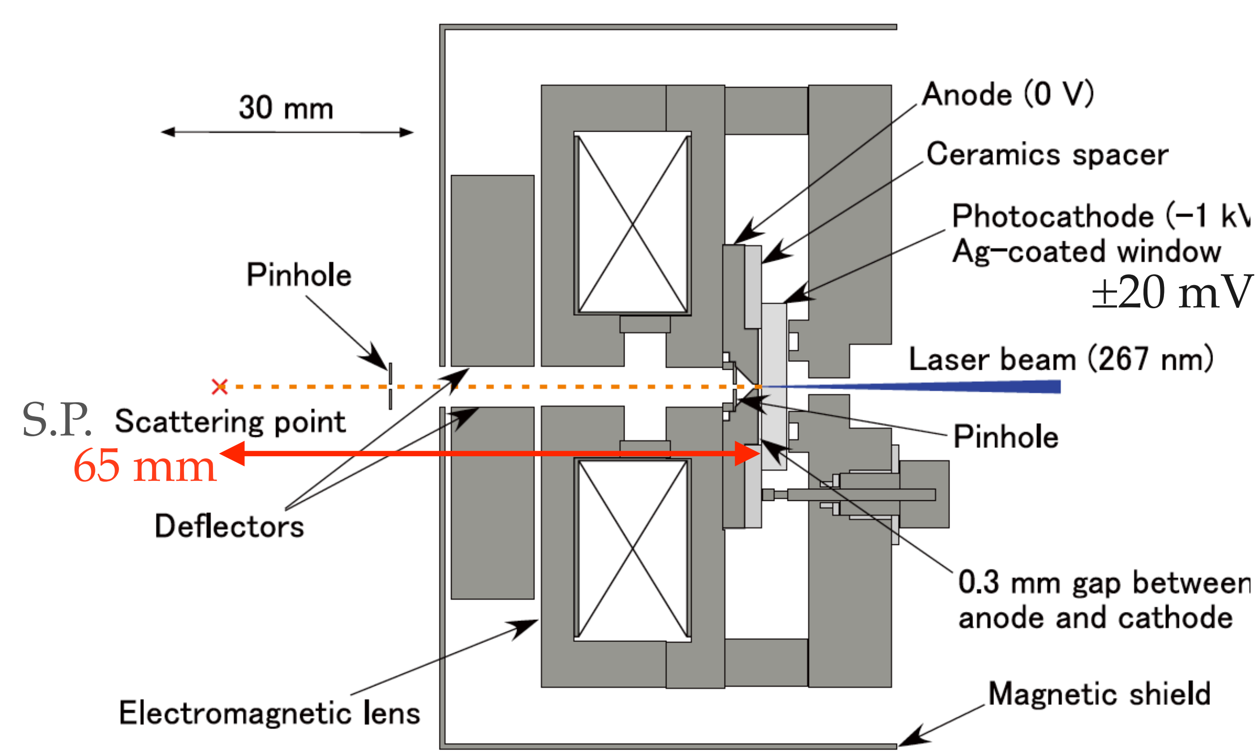

FIG. 3. (Color online) The cross section of the pulsed electron gun.

Experimental Setup

numbers in RSI2011
numbers in PRL2015+Suppl.

Beam stopper

Faraday cup <2.5°   Mo wire of 0.3 mmϕ

Toroidal electron analyzer

deceleration by -970V at the input lens

reacceleration by 970V at the output lens

⊿E = 0.7 eV   ⊿E = 0.3 eV

angular acceptance ±14°

Detector

MCP/Phosphor, 80mmϕ + CCD-Camera

gating duration: 140 nsec

electron counting

exposure 1 sec, ~10 electrons/sec

Background measurement with delay time of 100 psec

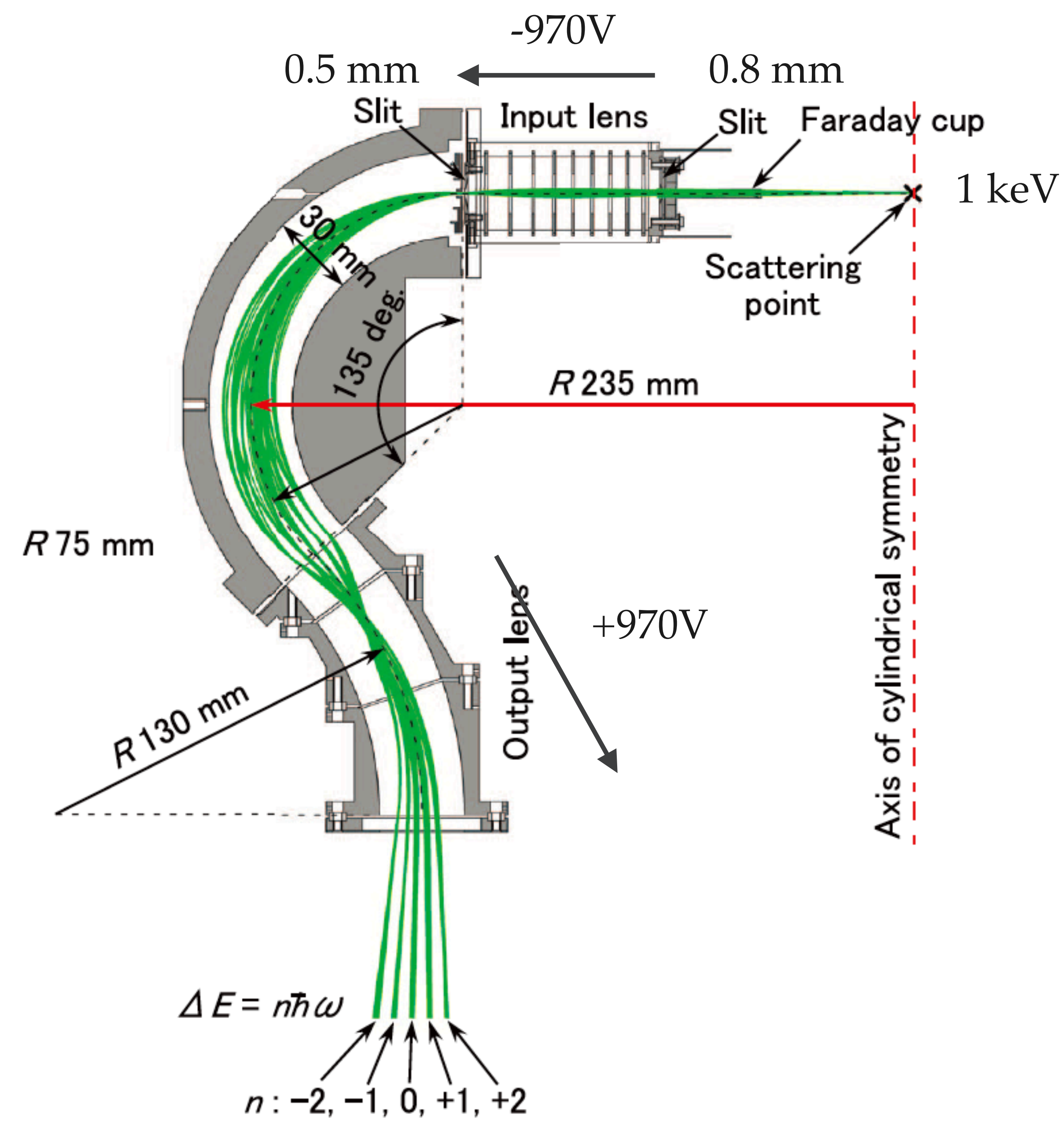

FIG. 6. (Color online) The cross section of the toroidal analyzer constructed for the LAES measurements, and the trajectories of the scattered electrons with the kinetic energy shifts of $-2\hbar\omega$, $-1\hbar\omega$, 0, $+1\hbar\omega$, and $+2\hbar\omega$.

Alignment

RSI2011

alignment checks, once in 6 hours

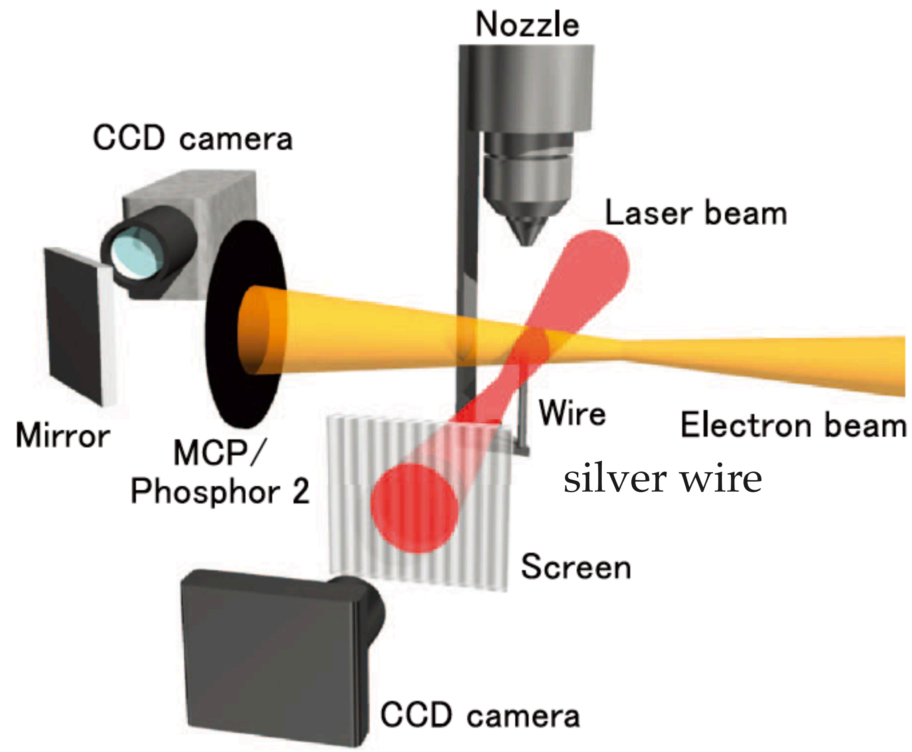

FIG. 7. (Color online) The experimental configuration for the alignment of the atomic beam, the electron beam, and the laser beam for LAES.

Temporal alignments

Electron beam image evolves in time due to the space-charge of electrons (thermally expanding) created on the silver-wire surface by multi-photon photoelectric emission by the laser.

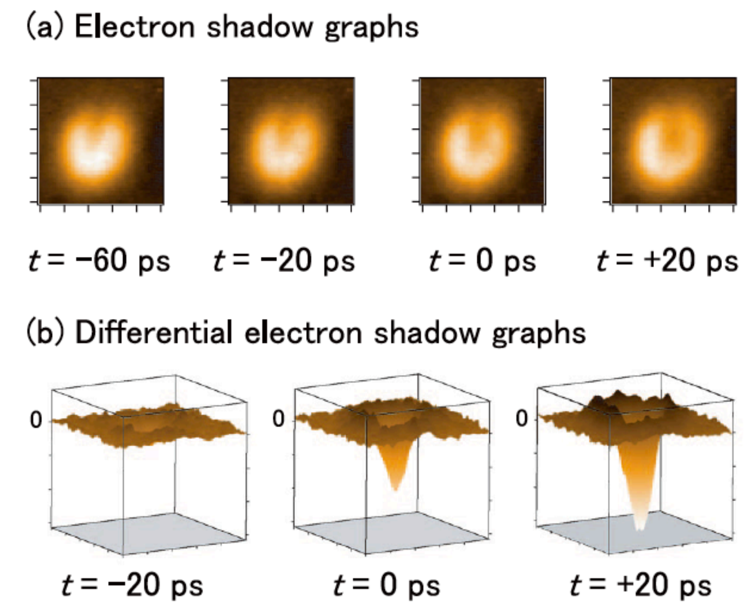

FIG. 10. (Color online) (a) The electron shadow graph images of the wire at the different delay time. (b) The 3D plots of the difference of the shadow graph images at $t = -20$, 0, +20 ps from the image at $t = -60$ ps.

Radial moment (due to expansion) as a function of the delay time. ⊿t ~ 1 psec

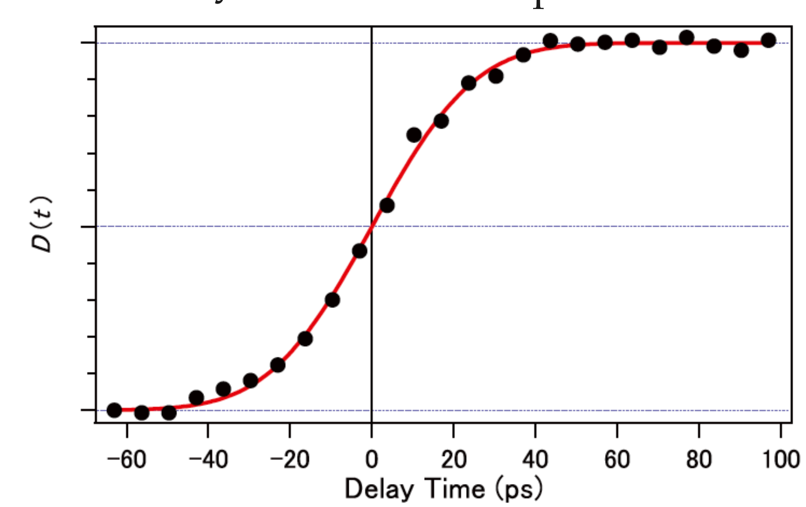

FIG. 11. (Color online) The delay time dependence of the first-order radial moment, $D(t)$ (Eq. (1)). Filled circles: the experimental results. Solid line: The result of a curve fitting of the experimental results with the function of Eq. (2).

$$D(t) \propto \int_{-\infty}^{\infty} \Theta(t - t') \exp\left(-\frac{t^2}{\tau^2} 4 \ln 2\right) dt'$$

electron pulse duration 45±5 psec

Spatial alignment

Electron shadow by the wire

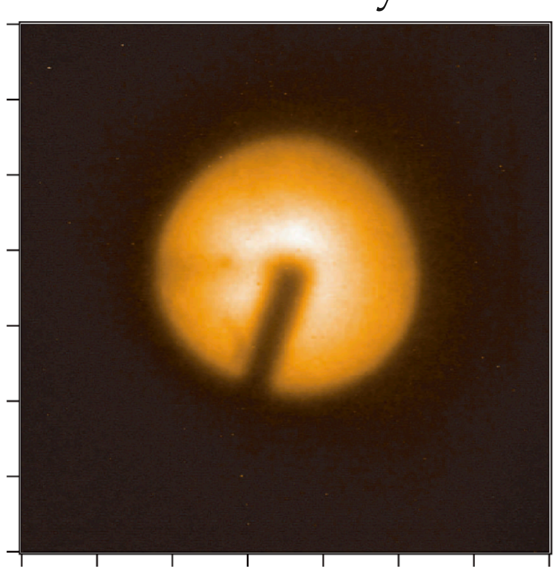

FIG. 9. (Color online) The observed electron shadow graph of the wire.

Laser shadow by the wire

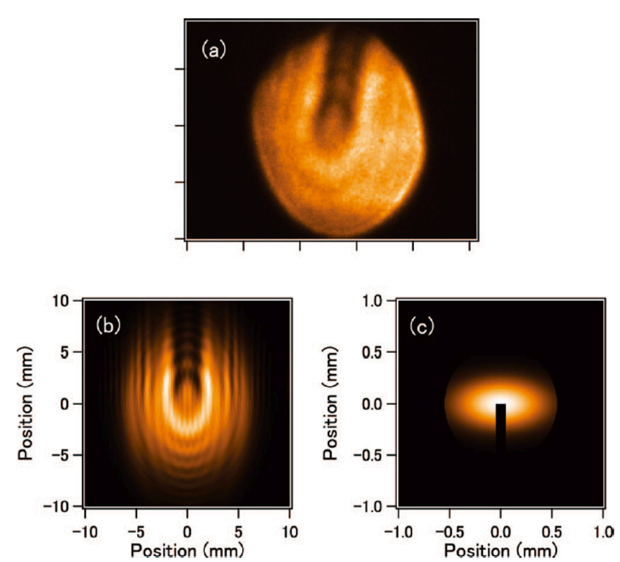

observed

simulation

FIG. 8. (Color online) The laser shadow graphs of the wire: (a) the observed shadow graph, (b) the calculated shadow graph, and (c) the initial beam profile at the scattering point adopted in the numerical propagation.

The shadows by the nozzle tip were also measured.

Results

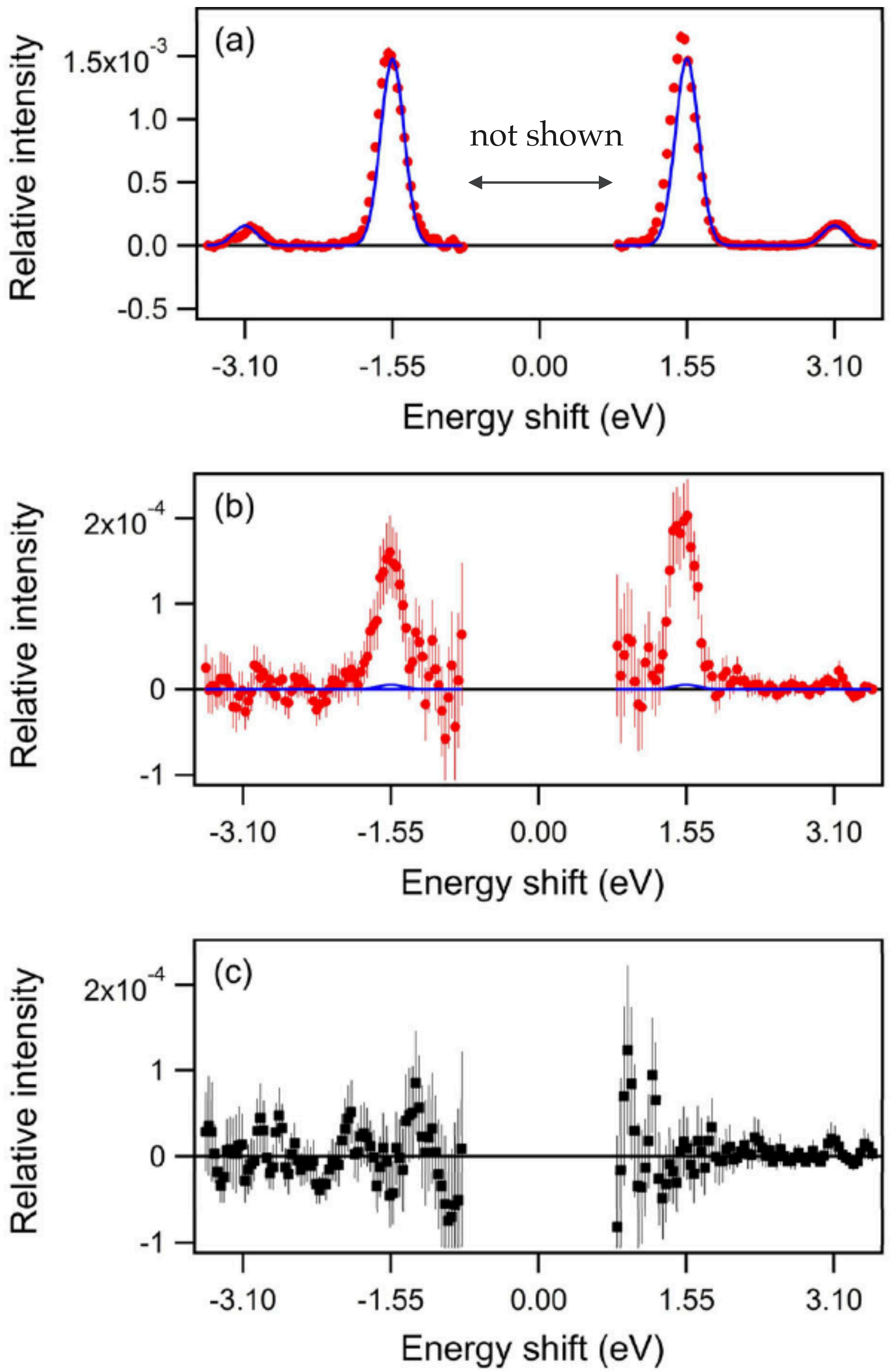

FIG. 2 (color online). The kinetic energy spectra of electrons

0.1-10.0°

vertical (z) pol.

blue: KW-model

LEAS signals (electron modulation) are clearly observed for $\pm\hbar\omega$ & $\pm 2\hbar\omega$

0.1-0.5°

vertical (z) pol.

blue: KW-model

0.1-0.5°

horizontal (y) pol.

no LEAS effect

Results

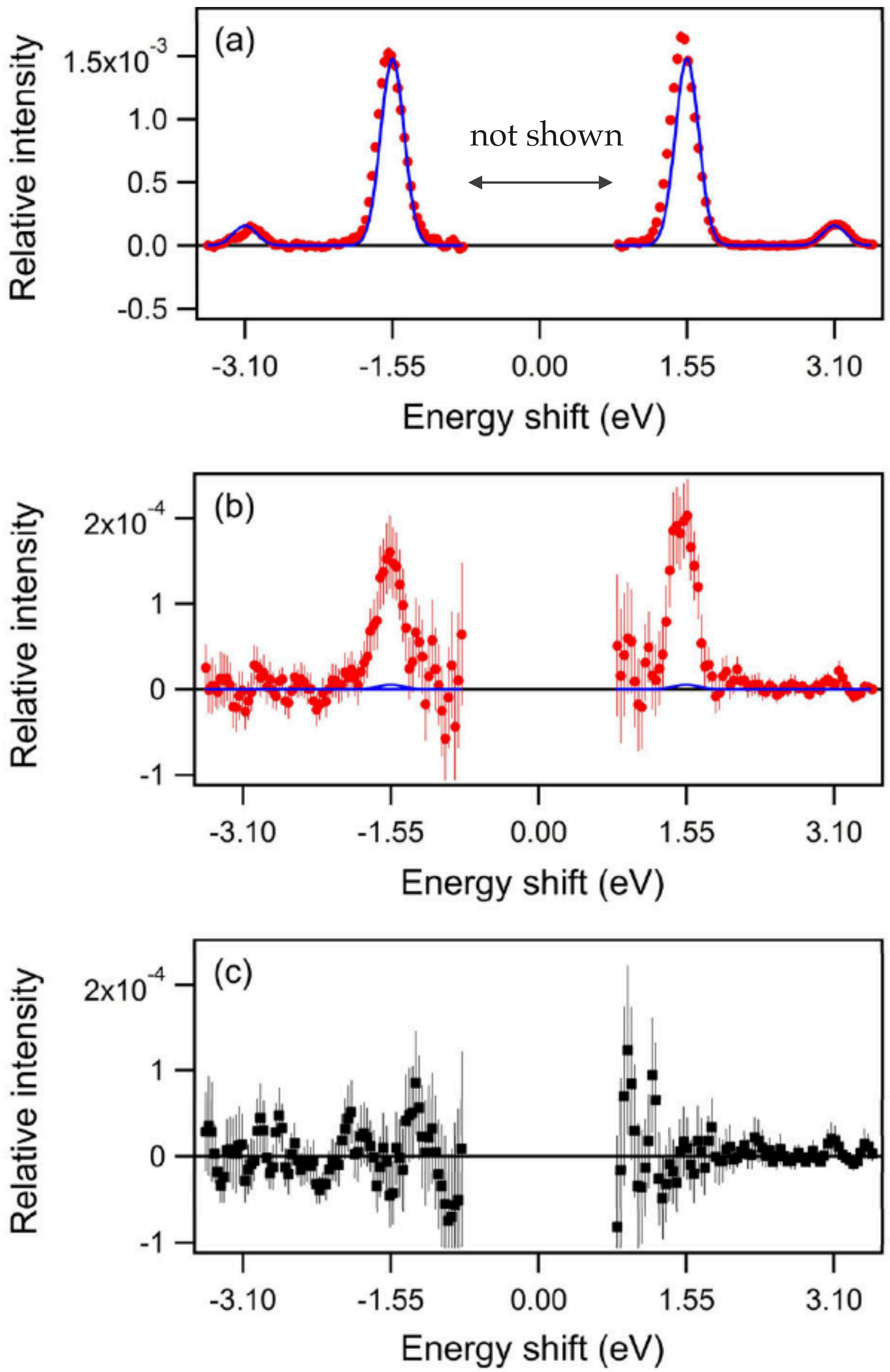

0.1-10.0°

vertical (z) pol.

blue: KW-model

LEAS signals (electron modulation) are clearly observed for $\pm\hbar\omega$ & $\pm 2\hbar\omega$

R. Kanya [36]

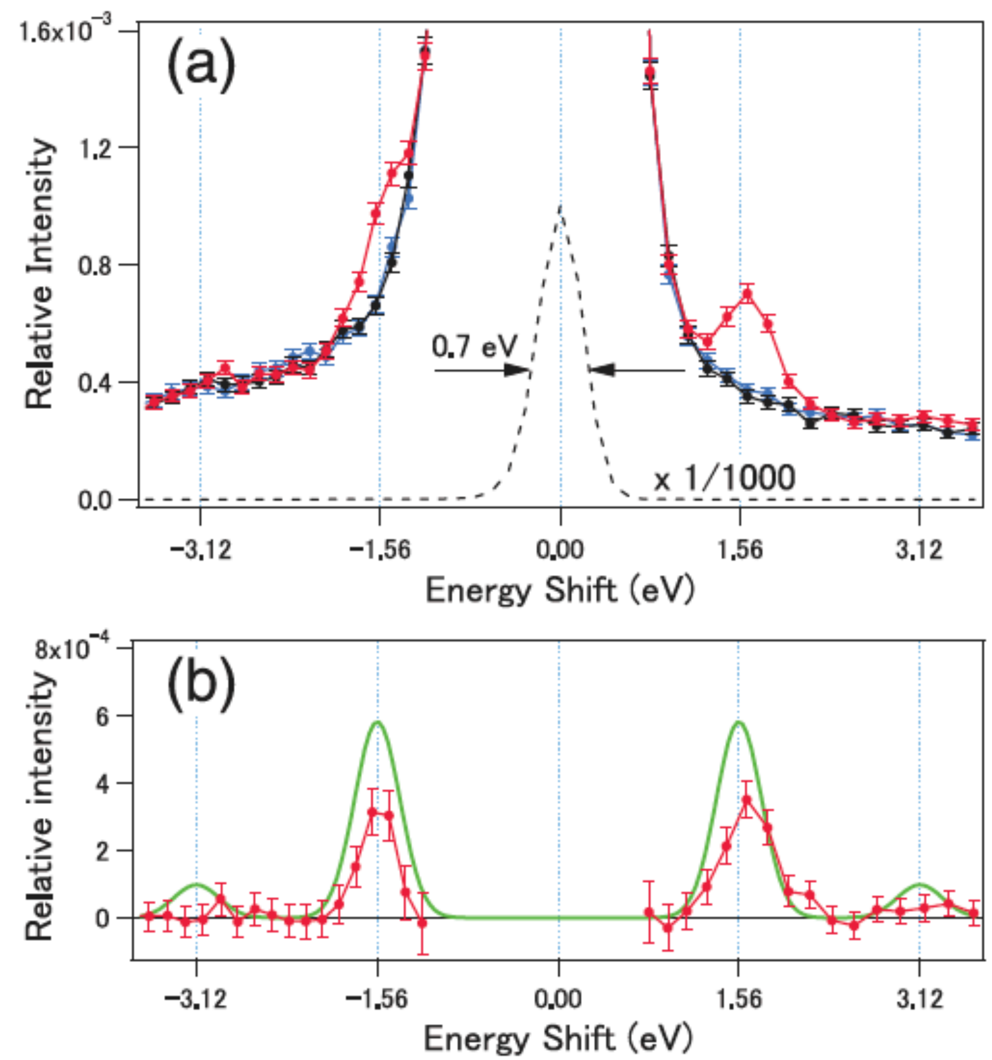

FIG. 2 (color online). The kinetic energy spectra of electroı

FIG. 3 (color). The energy spectra of relative intensities of

Results

Angular distributions

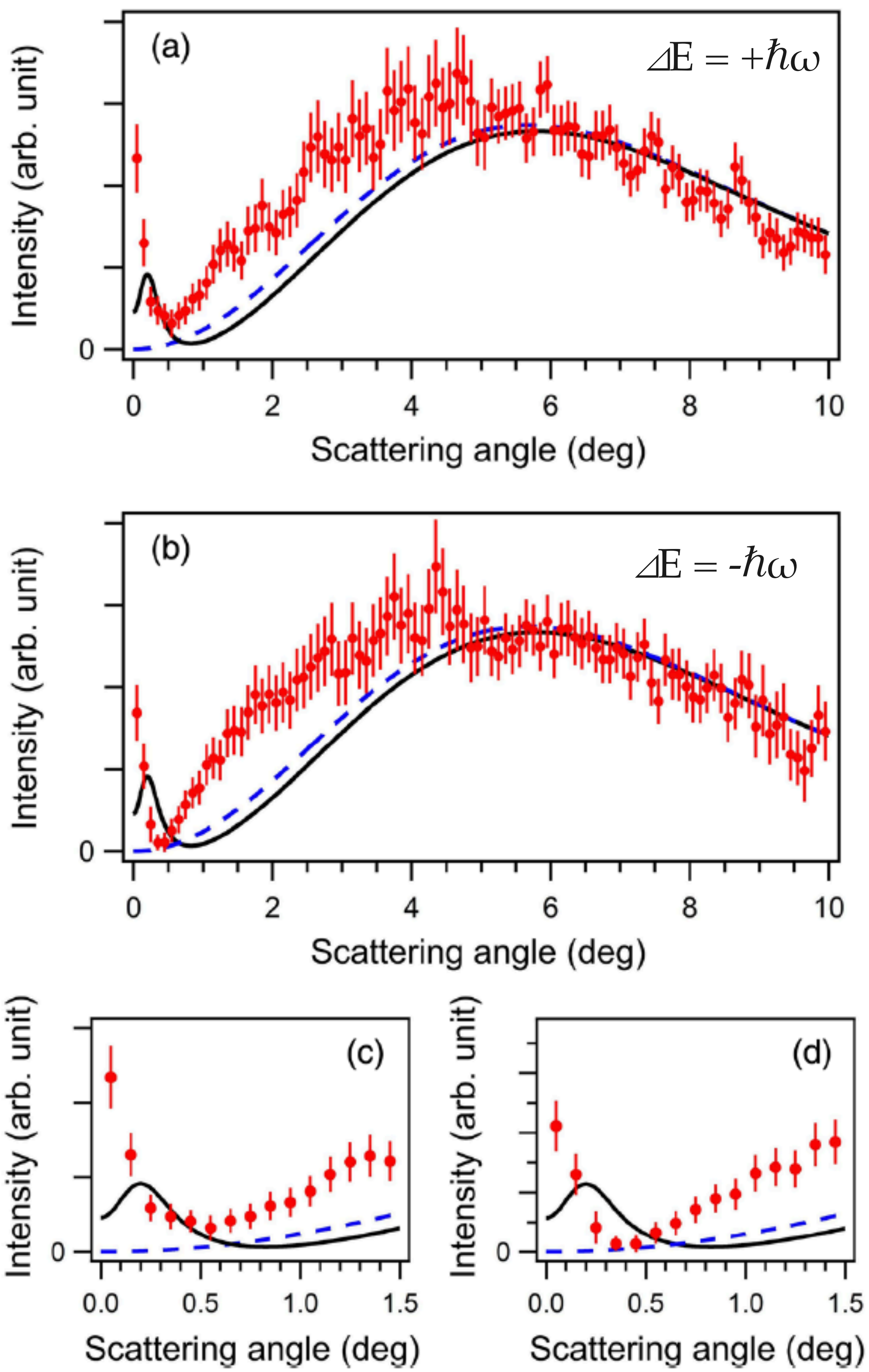

FIG. 3 (color online). The angular distributions of the LAES

light-dressing atom effect is observed

$$\frac{d\sigma_n^{KW}}{d\Omega} = \frac{|p_{f,n}|}{|p_i|} J_n^2(\xi) \frac{d\sigma_{el}^{exp,free}}{d\Omega}$$

exp. dcs is used for effectively including the higher-order effect in the Born approx.

blue dashed: KW-model

black solid: Zon-model

including the experimental conditions

electron beam emittance, resolution, etc

identical to the case of (a)

Enlarged figures

Results

Angular distributions

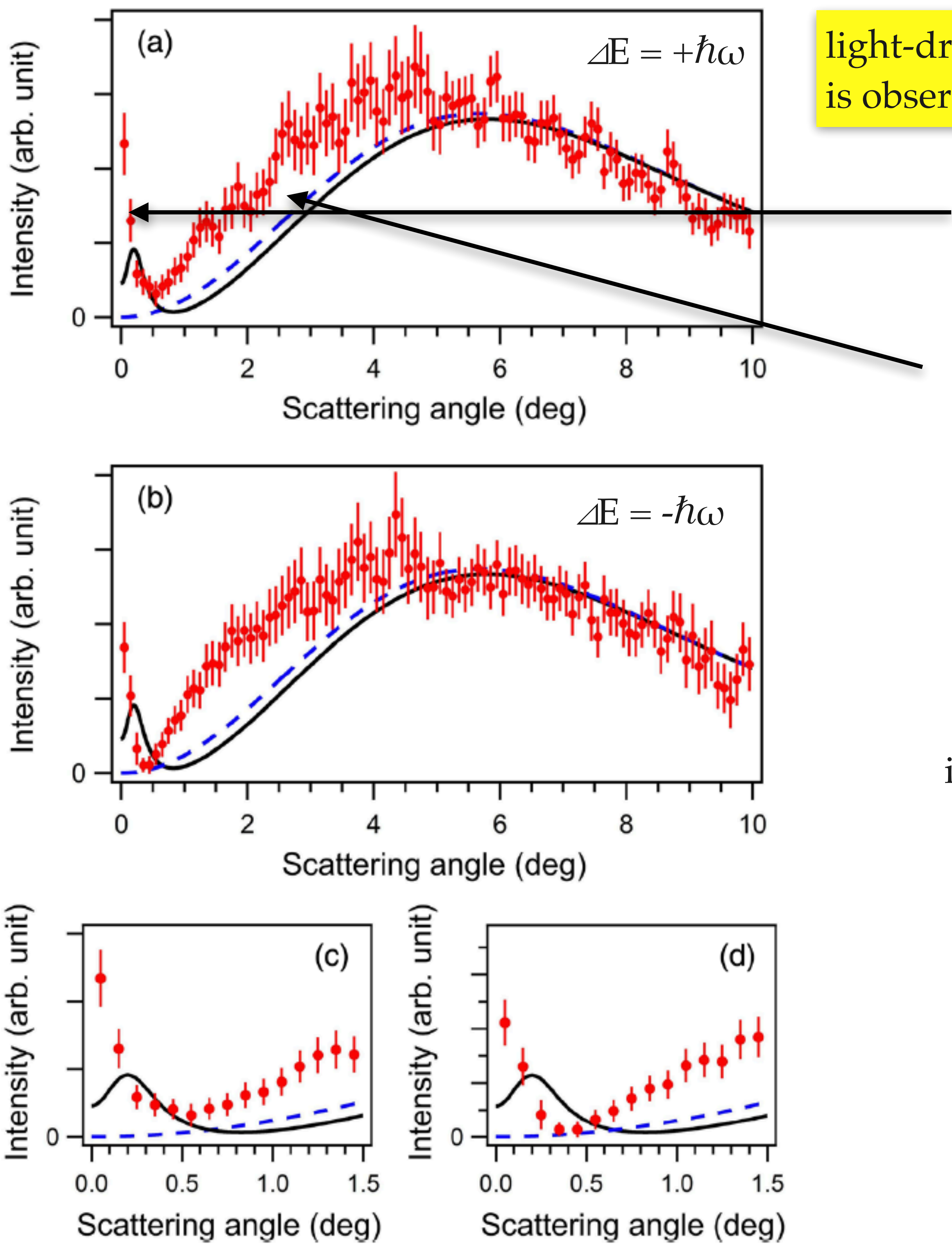

FIG. 3 (color online). The angular distributions of the LAES

light-dressing atom effect is observed

Discrepancy from the prediction at <0.2°:

from slight-misalignment?

Discrepancy from the prediction at 0.5<5.0°:

1) pol. of the atom by the projectile electron
2) deviation from the point dipole model
3) incomplete higher-order Born corrections

in supplemental material

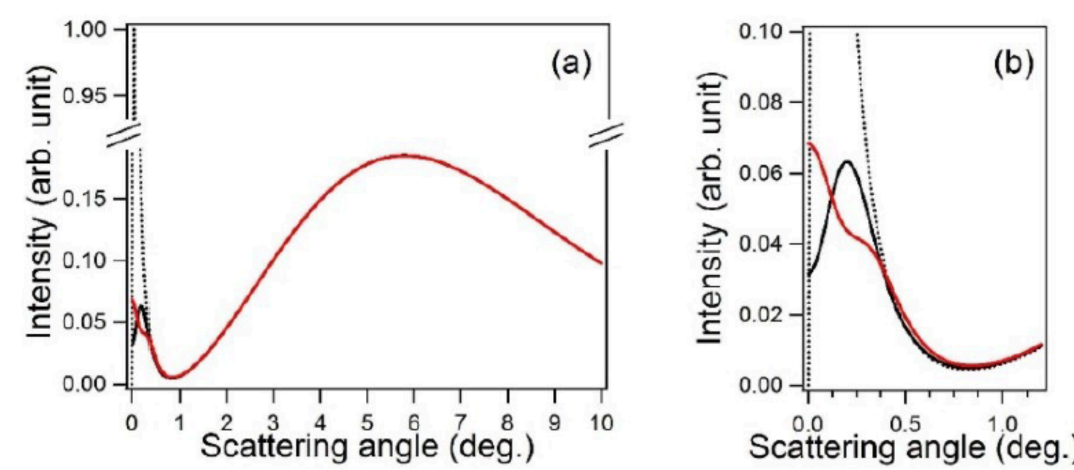

black dotted: Zon's model
black solid: +Mo wire, slit width, ang. res.
red solid: +displacement of the scattering point by ⊿z=50μm

Results

Angular distributions

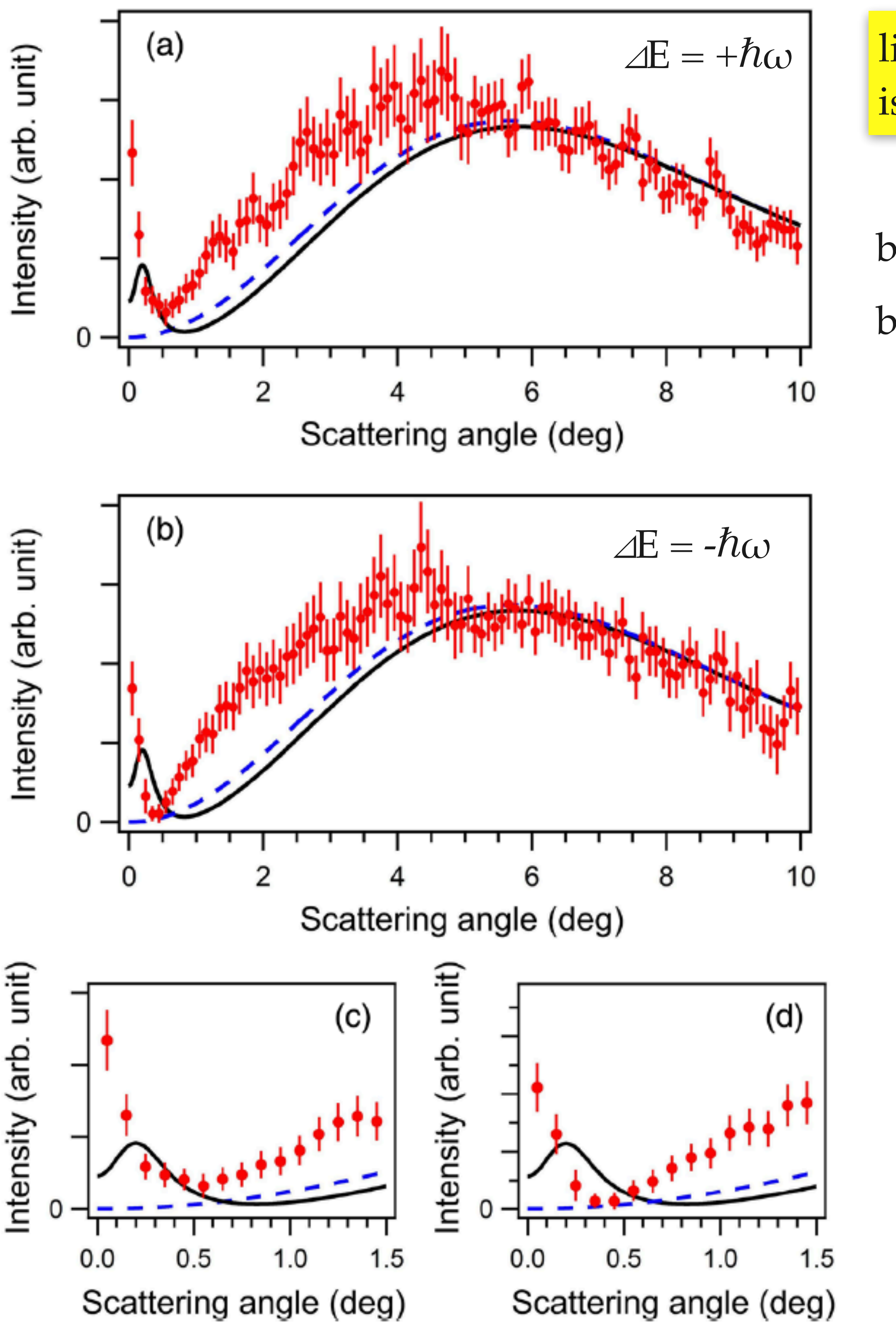

FIG. 3 (color online). The angular distributions of the LAES

light-dressing atom effect is observed

blue dashed: KW-model

black solid: Zon-model

including the experimental conditions

electron beam emittance, resolution, etc

$\Delta E = +2\hbar\omega$

no effect from the dressed-atom in the even n (due to the assumption of α_D)

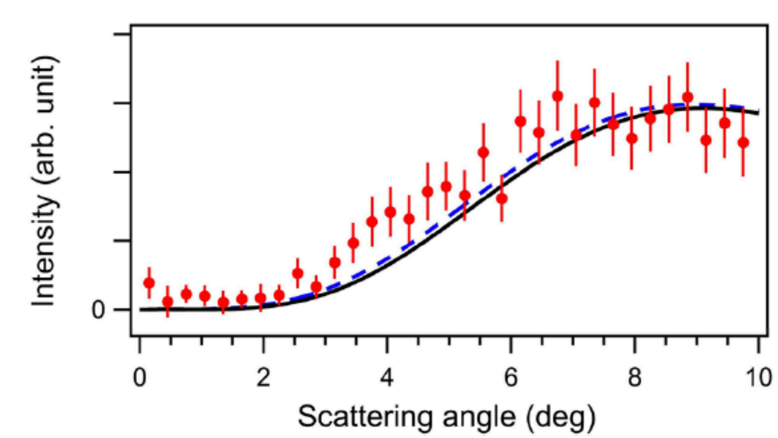

FIG. 4 (color online). The angular distribution of the LAES

Summary

Y. Morimoto, R. Kanya, and K. Yamanouchi, PRL**115**, 123201(2015)

In summary, we have observed the light-dressing effect in the target Xe atoms in the angular distributions of the LAES signals of $\Delta E = \pm\hbar\omega$, appearing as the peak structures at $\theta < 0.5°$. The result of the numerical simulation, in which the light-dressing effect is included based on Zon's model with the effective corrections of higher-order Born terms, is consistent with the recorded angular distribution exhibiting the peak profile at $\theta < 0.5°$. Through the analysis of experimental angular distributions of the LAES signals by referring to the results obtained by more elaborate numerical simulations, we will be able to extract information on the electron density distribution within a target atom dressed by an intense laser field.

— I have three more slides—

Later Publications

K. Ishida et al., PRA95, 023414(2017)

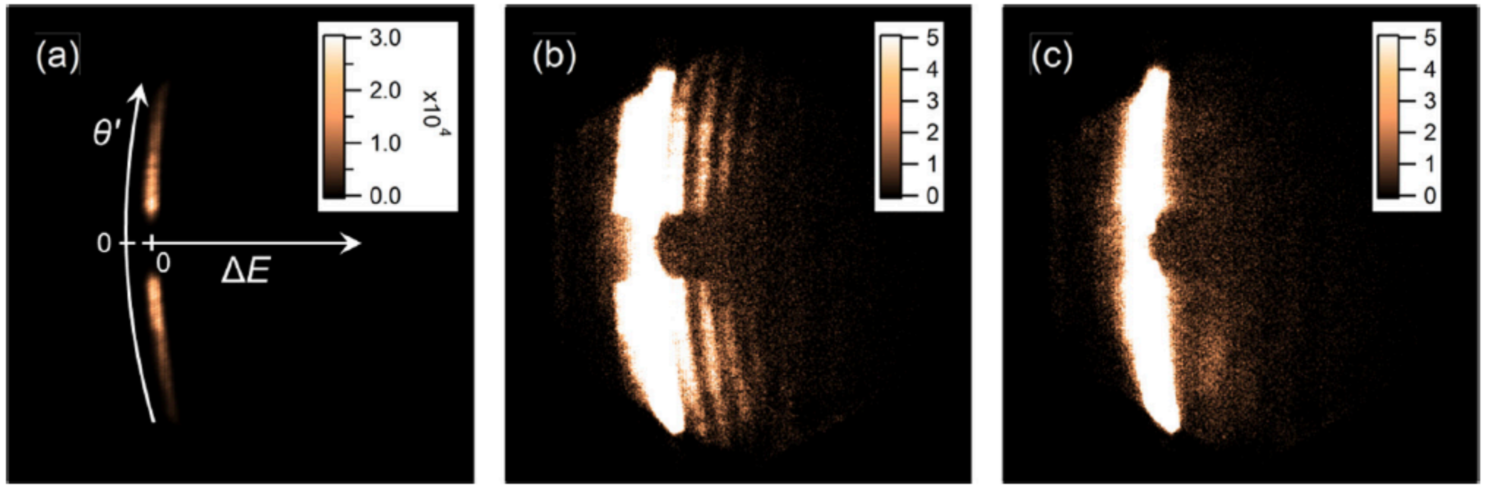

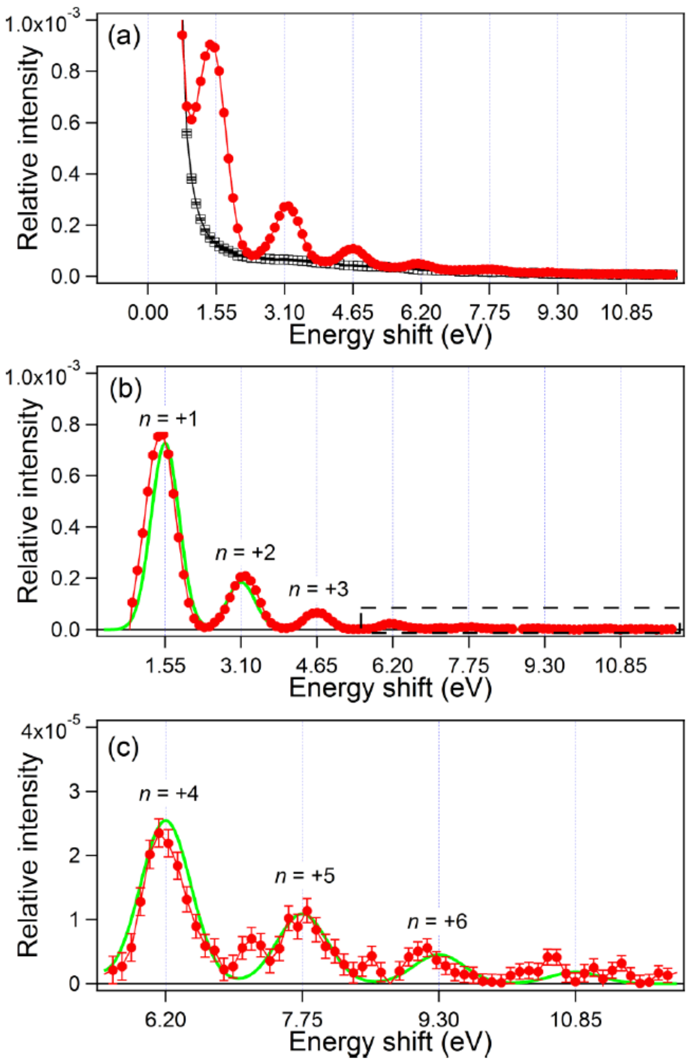

LAES (electron modulation) observed for up to n~6

Later Publications

Y. Morimoto and P. Baum, Nature Physics 14, 252(2018)

Diffraction and microscopy with attosecond electron pulse trains

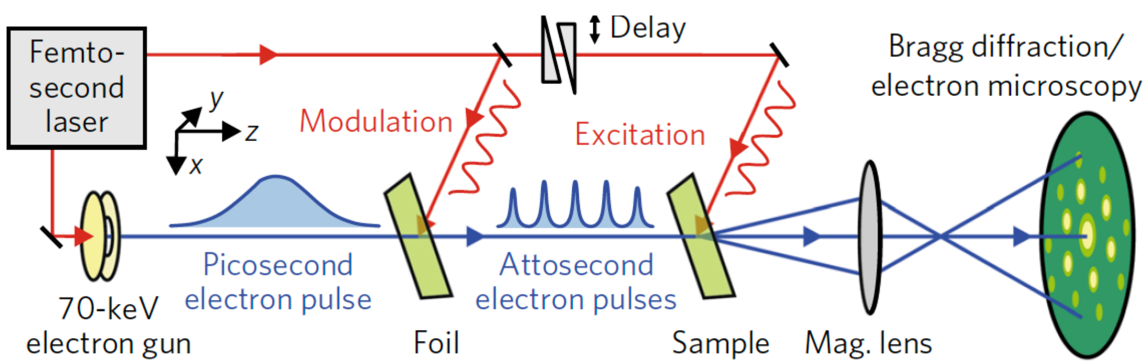

Fig. 1 | Concept and experiment. A photo-emitted picosecond electron pulse (blue) with a sub-atomic de Broglie wavelength is temporally modulated at a dielectric foil (green) by the optical cycles of a femtosecond laser (red) into a train of attosecond electron pulses (blue). Electron diffraction from a cycle-excited sample (green) can produce atomic resolution in space and time. Alternatively, real-space electron microscopy can reveal optical near-field vectors and phase delays with sub-cycle time resolution.

- creation of sub-femto-sec electron pulses
- atomic diffraction with sub-femto-sec resolution (with LEAS)

Investigation of the dynamical structure change of molecules (and chemical reactions) in the sub-femto-sec time order.

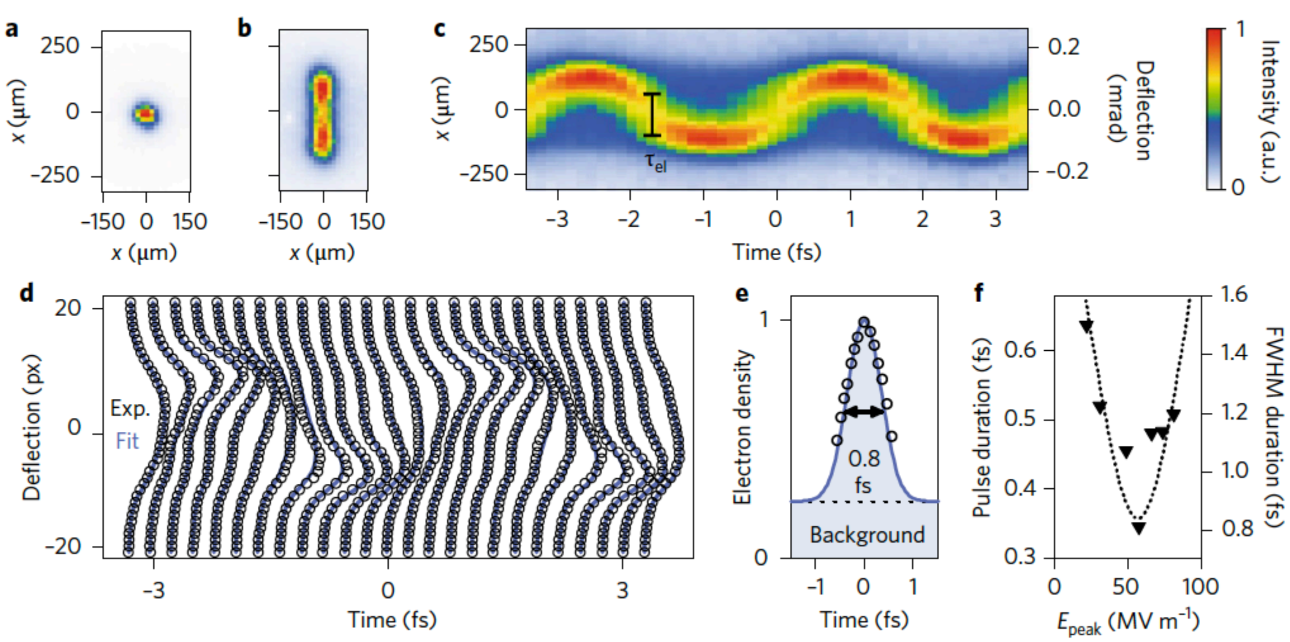

ig. 2 | **Attosecond electron pulses. a**, Basic electron beam profile. **b**, Streaking deflection of long electron pulses by optica

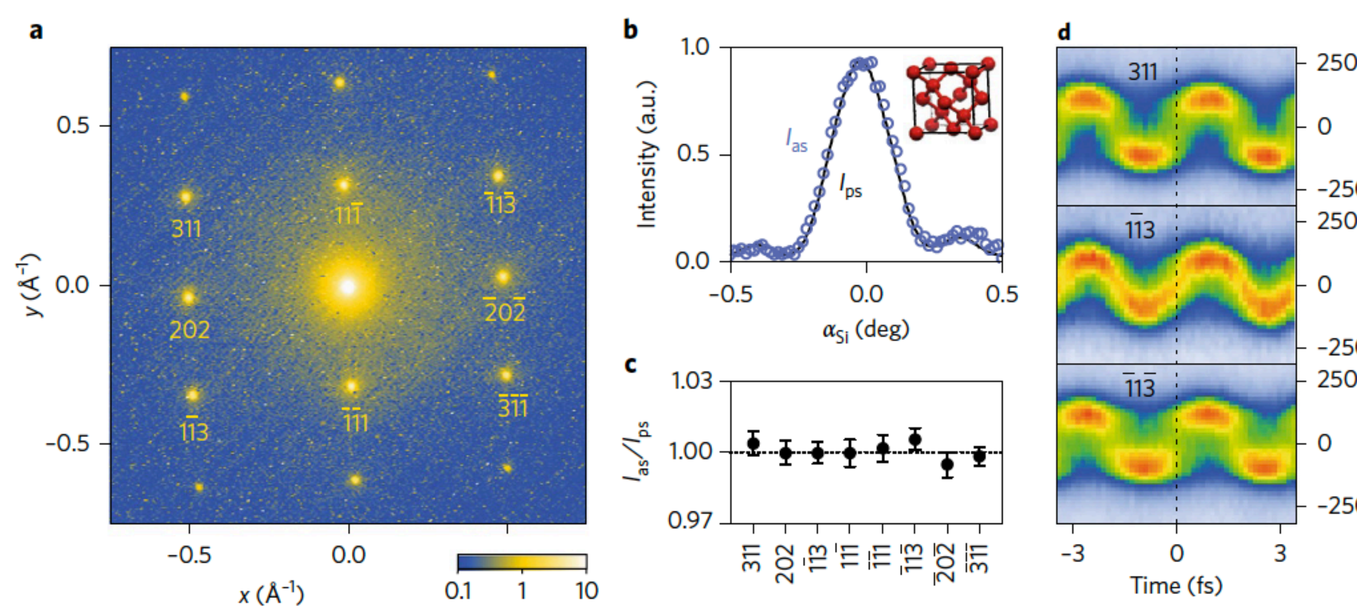

Fig. 3 | Atomic diffraction with attosecond electron pulses. a, Diffraction pattern of single-crystalline silicon, taken

Order of the light dressing effects comparison between the *e*-Xe and *p*-^{208}Pb cases

$$\frac{d\sigma_n^{KW}}{d\Omega} = \frac{|p_{f,n}|}{|p_i|} J_n^2(\xi) \frac{d\sigma_{el}^{free}}{d\Omega}$$

Kroll-Watson [6]

$$\frac{d\sigma_n^{Zon}}{d\Omega} = \frac{|p_{f,n}|}{|p_i|} |J_n(\xi) f_{el}^{free} - x\xi J_n'(\xi)|^2$$

Zon [38]

$$\xi = \frac{e\vec{E}_0 \cdot \vec{q}_n}{m_e \hbar \omega^2}$$

$$x = \frac{\alpha_D m_e^2 \omega^2}{2\pi\epsilon_0 q_n^2}$$

In the electron-atom collision case

1 keV (32 keV/c), 0.2° (4mr)
q = 0.13 keV/c
$\hbar\omega$ = 1.55 eV

1.5×10^{12} W/cm^2 → 3.4×10^{9} V/m
α_D = 4.04 Å^3

$\xi = 0.07$

$x = 4\times10^{-8}$ m

$(x\xi)^2 = 8\times10^{-18}$ m^2

In the proton-^{208}Pb scattering case

very-uneasy → 65 MeV (355 MeV/c), 0.2° (4mr)
q = 1.3 MeV/c
$\hbar\omega$ = 1.55 eV

1.5×10^{12} W/cm^2 → 3.4×10^{9} V/m
α_D = 20 fm^3
] can be enlarged

$\xi = 0.4$

$x = 7\times10^{-14}$ m

$(x\xi)^2 = 7\times10^{-28}$ m^2 = 7 b

Thank you

for your attention